

Hydroconversion of Furfural over Cu-Cr/SiO₂ Nanocatalysts: A Comparative Study

M. Ghashghaee^{1,2*}, S. Shirvani^{1,2}, V. Farzaneh^{1,2}

¹ Faculty of Petrochemicals, Iran Polymer and Petrochemical Institute, P.O. Box: 14975-112, Tehran, Iran

² Biomass Conversion Science and Technology (BCST) Division, Iran Polymer and Petrochemical Institute, P.O. Box: 14975-115, Tehran, Iran

ARTICLE INFO

Article history:

Received: 2017-07-11

Accepted: 2017-10-09

Keywords:

Hydrogenation,
Furfuryl Alcohol,
Nano Silica,
Promoter,
Impregnation,
Chromium,
Biomass,
Biomonomers

ABSTRACT

Furfural is one of the most promising chemical platforms with bright perspective with respect to the production of bio-based chemicals and fuels from lignocellulosic material. Globally, the majority of the biomass-derived chemicals are converted into furfuryl alcohol, a building block in polymers industry. The vapor-phase hydrogenation of furfural over copper species dispersed on two types of silica (bulk-type and nano-sized) supports with or without chromium as a promoter was studied for the first time. The catalysts were synthesized via impregnation method and operated under mild hydrogenation reaction conditions. The results represented that the catalytic performance of the nano-sized silica-supported catalyst was better in terms of furfural conversion, furfuryl alcohol yield and selectivity than that of the bulk-type silica after a 4-hour operation. However, by incorporation of chromium as a promoter, the bulk-type silica-supported catalyst exhibited an improved performance during the whole run length (higher than 82 % and 96 % of furfural conversion and furfuryl alcohol selectivity, respectively).

1. Introduction

Nowadays, decline of fossil reservoirs and growing environmental pollution in combination with increasing energy demands have fueled investigations to find an appropriate alternative to the fossil-based processes [1-2]. Biomass is one of the most valuable sources that can play a vital role in supplying energy and important chemicals [3-10]. Among those biomass-based materials, furfural is considered as one of the most promising platforms with bright future due to

a relatively facile production process directly from lignocellulosic material and also its ability to be converted catalytically to a vast range of biofuels, solvents, and noteworthy chemicals such as furfuryl alcohol, 2-methylfuran, furan, tetrahydrofuran, methyltetrahydrofuran, pentanediols, γ -valerolactone, furfurylamine, maleic acid, and so on through different pathways [1-2, 11-14]. The furfural hydrogenation process can be performed in the gas or liquid phases; however, the gas-phase hydrogenation of

*Corresponding author: m.ghashghaee@ippi.ac.ir

furfural finds more preferences due to its milder reaction conditions and convenience of handling [11, 15-16]. Furfuryl alcohol is one of the most significant products of the hydrogenation process with wide applications in polymer industries and also is an intermediate in the production of lubricants, ascorbic acid, dispersing agents, and lysine [1-2, 13, 17-20]. By applying copper-based catalysts, the hydrogenation process mainly proceeds to form furfuryl alcohol [21]. So far, different copper catalysts have been proposed for this process: carbon-supported copper [22], silica- or magnesia-supported copper [23-26], Raney nickel [27-28], nickel amorphous alloys [29-30], copper–magnesia [15, 23, 31-33], copper zinc oxides [34], titania-supported copper and promoted copper [35-36], mixed copper zinc oxides with aluminum, manganese, and iron [37], and homogenous mixture of rhodium, ruthenium, and platinum [16, 38-39]. Silica-supported copper is one of the recently proposed catalysts that provides high furfural conversion and also great selectivity towards furfuryl alcohol [11, 24, 40-41].

The promoting effect of Cr on the performance of Cu/SiO₂ catalysts awaits investigation. Moreover, the type of silica support has not been changed in the previous studies to explain possible consequences. The present work then attempts to highlight the effects of changing the silica support (nano-sized or bulk-type) as well as the introduction of chromium as a promoter on the performance of silica-supported copper catalysts in the gas-phase hydrogenation of furfural.

2. Experimental

2.1. Materials

Cu(NO₃)₂·3H₂O (Merck, 99.5 %), commercial

silica (Sigma-Aldrich, 34–45 μm, ~ 600 m²/g) and nano silica (NanoSav, 20–30 nm, 193 m²/g) supports were used as starting materials. Cr(NO₃)₃·9H₂O (97 %) was purchased from Scharlau. All chemicals were used without any further purification. The material employed for studying the catalytic activity included furfural (98.90 %, Merck) and high purity hydrogen (99.99 %) and nitrogen (99.99 %).

2.2. Catalyst preparation

Commercial macro-sized and nano-sized silica were applied as the catalyst support. The loadings of copper and chromium were 10 wt % and 5 wt % for all catalyst samples, respectively. An aqueous solution of copper nitrate and chromium nitrate was slowly impregnated onto various silica supports under mild stirring conditions. The doped catalysts were dried at 150 °C for 15 h and, subsequently, calcined at 550 °C for 5 h to obtain the final oxide catalysts. In this paper, the synthesized catalysts with Cu/SiO₂ (bulk-type), Cu-Cr/SiO₂ (bulk-type), Cu/SiO₂ (nano-sized), and Cu-Cr/SiO₂ (nano-sized) were denoted as CS1, CS2, CS3, and CS4, respectively.

2.3. Catalyst characterization

The XRD patterns of the catalysts were measured by a Siemens, D5000 diffractometer using Co K α radiation in the range of 10–80 ° with a step size of 0.02 ° and an exposure time of 2 s per step. The scanning electron microscopic (SEM) images were obtained on a Tescan instrument using Au-coated sample with an acceleration voltage of 20 kV. The component distribution and analysis on the surface of the samples were studied by energy dispersive spectrometry (EDS) using Tescan instrument. A Quantachrome Chem-BET 3000 sorption

analyzer measured the N₂ physisorption data for the Brunauer–Emmett–Teller (BET) analysis at 77 K. The samples were degassed at 393 K for 3 h before the measurements.

2.4. Catalyst activity

The furfural hydrogenation process over silica-supported catalysts was conducted in a tubular quartz reactor with 10 mm internal diameter. The pelletized catalyst was loaded between two plugs of quartz wool. The reactor was placed in an electrical furnace which supplied the required energy for the reaction. Prior to the reaction, the catalyst was reduced in a diluted hydrogen flow with total rate of ~ 6 Lg⁻¹h⁻¹ at 523 K for 3 h. After reduction, the catalyst was cooled down to the reaction temperature in pure hydrogen. Then, furfural was fed continuously into the reactor using a microfeeder. The reactions were carried out at a temperature of 453 K and space velocity (WHSV) of 1.7 h⁻¹ under atmospheric pressure with a hydrogen-to-feedstock volumetric ratio (HFR) of 10. A gas chromatograph (GC) equipped with a capillary column and an FID was applied for analysis of collected products every few minutes. The carbon balance was generally better than 95 % in all experiments unless otherwise stated. The performance data were measured using the following equations:

$$\text{Conversion (\%)} = \frac{\text{moles of furfural consumed}}{\text{moles of furfural fed}} \times 100 \quad (1)$$

$$\text{Selectivity (mol \%)} = \frac{\text{moles of desired product}}{\text{moles of furfural consumed}} \times 100 \quad (2)$$

$$\text{Yield (mol \%)} = \frac{\text{moles of desired product}}{\text{moles of furfural fed}} \times 100 \quad (3)$$

3. Results and discussion

Fig. 1 illustrates the performance results of the vapor-phase hydrogenation of furfural in terms of furfural (FF) conversion, furfuryl alcohol (FFA) yield, and selectivity of the four synthesized catalysts. As is obvious in this figure, CS1 catalyst exhibited the poorest catalytic performance among others. Although it had satisfactory FFA selectivity (above 88 % after 4 h of reaction), the conversion of furfural and yield of furfuryl alcohol for this catalyst were respectively lower than 13.1 % and 9.1 % during the operation. With the addition of chromium as a promoter to this catalyst, the results improved significantly, particularly in terms of conversion of FF and yield of FFA which amounted to 82.3 % and 79.3 %, respectively, after 4 h of operation (see Fig. 1, the CS2 panel). In addition, the selectivity towards FFA for this catalyst increased gradually from 91.4 % within the first hour of operation to 96.2 % at the end. Clearly, the CS3 catalyst with FFA selectivity, FF conversion, and FFA yield higher than 91 %, 38 %, and 35 % showed, overall, a remarkably better performance in comparison with CS1. Moreover, Fig. 1 elucidates that CS4 was the most selective catalyst among the others, the selectivity of which was more than 97.1 % at the entire range of operation. It also had the highest FFA yield and FF conversion in the first hour of the hydrogenation process (90.9 % and 93.5 %, respectively); however, the amount of these variables decreased rapidly and reached 56.5 % and 56.4 % during the 4 h test. The poor sustainability of this catalyst can be regarded as its main drawback. Generally, the most durable catalysts are CS2 and CS3 (see Fig. 1).

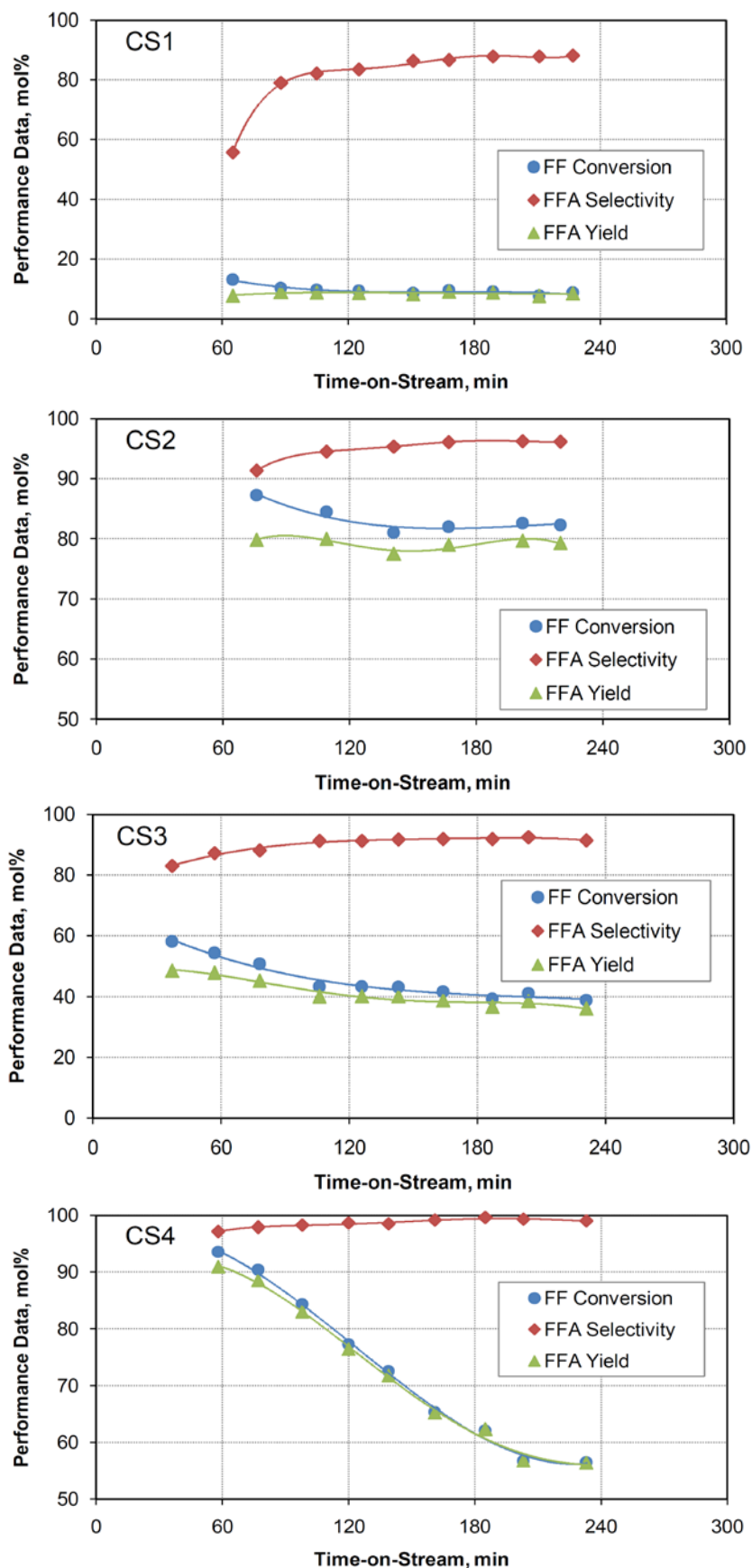


Figure 1. The performance data of the synthesized catalysts in the vapor-phase hydrogenation of furfural at 453 K, 1 atm, WHSV of 1.7 h⁻¹, and HFR of 10.

Considering all aspects together, one can deduce that CS2 (chromium-promoted catalyst with the bulk-type silica as the support) had the best overall performance in the furfural hydrogenation process. Moreover, the incorporation of chromium as a promoter in the bulk-type silica-supported catalyst improved its performance dramatically (compare CS1 and CS2 graphs in Fig. 1) as also partially seen for the nano-sized silica-supported catalysts. More strictly, although the incorporation of chromium in this type of catalyst enhanced all performance indices, particularly the FF conversion and FFA yield, it gave rise to a significant decrease in the durability of the catalyst (compare the CS3 and CS4 graphs).

A schematic diagram of the reactions leading to the main products in this work is shown in Fig. 2. Moreover, Fig. 3 presents the average amounts of the important byproducts produced during 4 h of operation in the furfural hydrogenation process. As is clear in

this figure, CS1 produced maximum amounts of byproducts (18 % in total), particularly 2,2-methylenebisfuran (MBF), 5-methylfurfural (MFF), δ -valerolactone (DVL), 2-acetylfuran (AF), and 2-(2-furylmethyl)-5-methylfuran (FMMF). In addition, it also produced trace amounts of cyclopentanone (CPON), 5-methylfurfuryl alcohol (MFFA), and γ -valerolactone (GVL). Consequently, the catalyst was not so selective towards FFA (see Fig. 1). CS2 produced more disparate, yet less, amounts of byproducts (3 % in total), the main byproducts of which included 5-methylfuran (MF), FMMF, CPON, and MBF. The important byproducts produced over CS3 catalyst included 1,5-pentandiol (15PDO), FMMF, and CPON. This catalyst also formed MF, furfuryl ether (FFE), MFF and AF in lower amounts. The CS4 catalyst showed the minimum amount of byproducts in accordance with its high selectivity towards FFA (Fig. 1). Besides FFA, it mainly produced 15PDO and MFF.

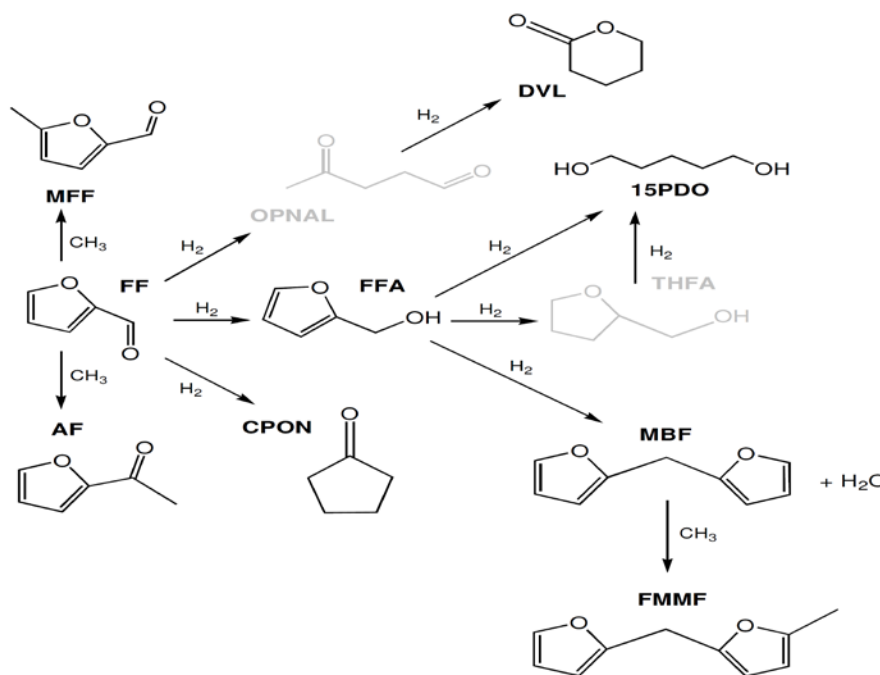


Figure 2. The overall reaction scheme for the main products and byproducts (with selectivity higher than 1 %) obtained over the silica-supported catalysts.

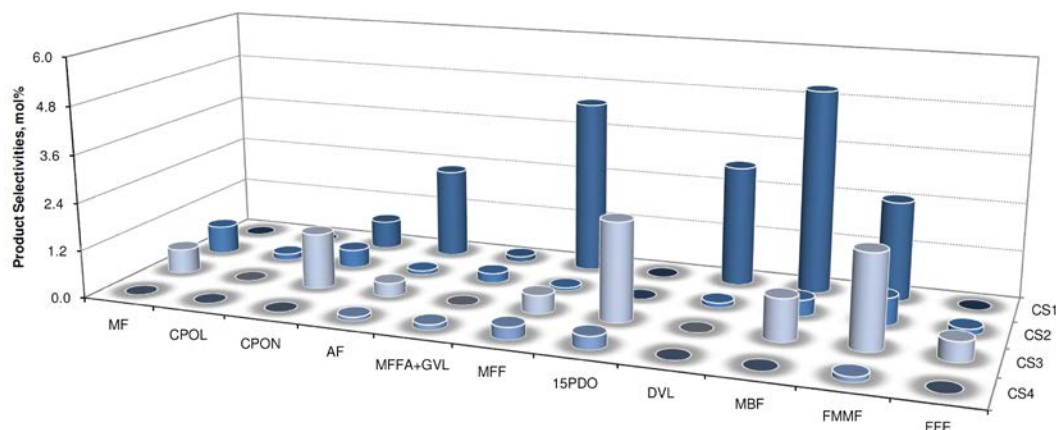


Figure 3. The major byproducts of CS1, CS2, CS3, and CS4. The reaction conditions were 453 K, 1 atm, WHSV of 1.7 h^{-1} , and HFR of 10.

To gain more insight into the origin of these performance differences, the XRD patterns of the synthesized catalysts on different supports were obtained (Fig. 4). As shown in this figure, the fabricated catalysts showed different patterns and peak intensities. All synthesized catalysts possessed CuO phases ($2\theta = 39^\circ, 41.5^\circ, 45^\circ, 54.1^\circ, 57.5^\circ, 63^\circ, 69^\circ, 73^\circ$ and 78.82° (JCPDS 45-0937)). In the Cr-containing samples, i.e., CS2 and CS4, CuCr_2O_4 phase was also detected (weak signals at $2\theta = 34.5^\circ, 37^\circ, 43.7^\circ, 66.5^\circ,$ and 77° are attributed to the CuCr_2O_4 phase (JCPDS 72-1212)). The crystallite sizes of the CuO for the four samples are shown in Table 1 as calculated by the Scherrer formula. These data showed that the copper oxide crystallite sizes of Cr-free catalysts, CS1 and CS3, were

larger than those of Cr-containing counterparts. Moreover, using bulk silica prompted a catalyst with larger crystallite size. According to Fig. 4, a decrease in the intensities of the peaks happened after the addition of the Cr promoter. Moreover, the widths of the obtained XRD peaks showed a broadening with the addition of the promoter. The superior catalytic activity of CS2 and CS4 samples for the hydrogenation of furfural can be attributed to the interaction between Cu and Cr species in CuCr_2O_4 catalysts, as similarly stated in the literature [42-43]. The small peaks of CuO phases in CS2 and CS4 diffraction patterns indicate the high dispersion of the catalytic species on SiO_2 supports, which could result in the observed satisfactory catalytic activity [44].

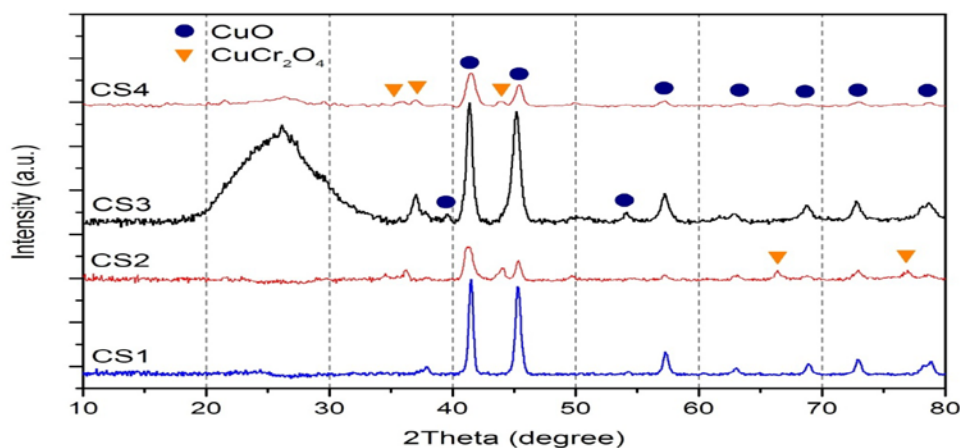


Figure 4. XRD patterns of the synthesized catalysts.

Table 1

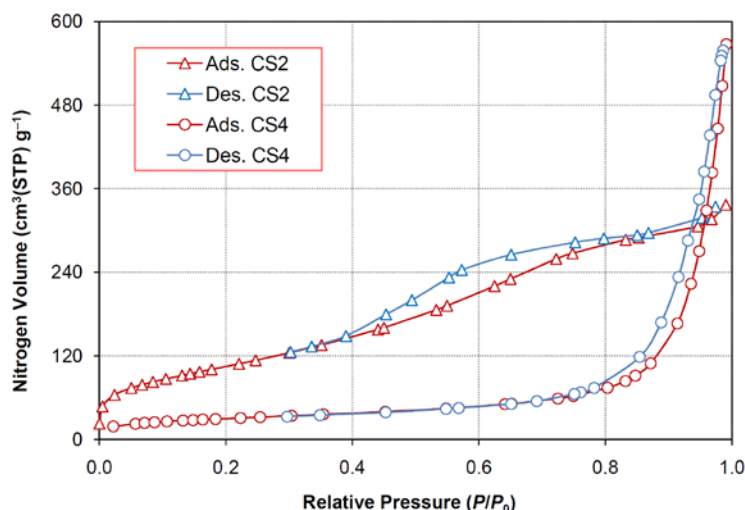
Textural properties of the impregnated catalysts.

Sample	CuO crystallite size (nm)	BET surface area (m ² /g)
CS1	23.3	453.7
CS2	12.6	477.4
CS3	18.0	133.5
CS4	12.3	107.4

The measured BET surface areas of all fabricated catalysts are tabulated in Table 1. It was observed that CS2 sample had the highest surface area (477.4 m²g⁻¹) followed by CS1 (453.7 m²g⁻¹), CS3 (133.5 m²g⁻¹), and CS4 (107.4 m²g⁻¹). As obvious, the addition of the Cr promoter affected the BET surface areas of the final catalysts. Although the addition of Cr promoter in CS3 decreased the surface area of the final catalyst, CS4, it had an opposite effect in the case of CS1; CS2 exhibited higher surface area than CS1. These observations together with the catalytic results elucidated that the surface area has a remarkable impact on the catalytic activity, yet cannot justify it as an the only factor.

Fig. 5 illustrates the N₂ adsorption-desorption isotherms as well as BJH plots of CS2 and CS4 as the representatives of two types of supported catalysts. According to the IUPAC classifications [45], CS4 showed type II of adsorption isotherm with the hysteresis loop of type H3, and CS2 presented type IV of

adsorption isotherm and the hysteresis loop of type H4. The former type is usually allocated to materials with relatively large pores or without any porous structure, while the latter is attributed to the systems with mesoporous structure where their filling and emptying occur through capillary condensation. These results are reasonable as the nano-sized silica particles have high adsorption capacity on their external surface area and inter-particle spaces. On the other hand, the micro-sized silica support in CS2 was highly porous, providing a huge internal surface area for the dispersion of both active sites and promoter species. When the types of hysteresis loops are concerned, the hysteresis loop of CS4 could be assigned to the aggregates of particles or materials with slit-shaped pores. Regarding CS2, slit-shaped pores are assigned except that, in this case, the pore size distribution is mainly placed in the range of micropores (see Fig. 5, lower panel).



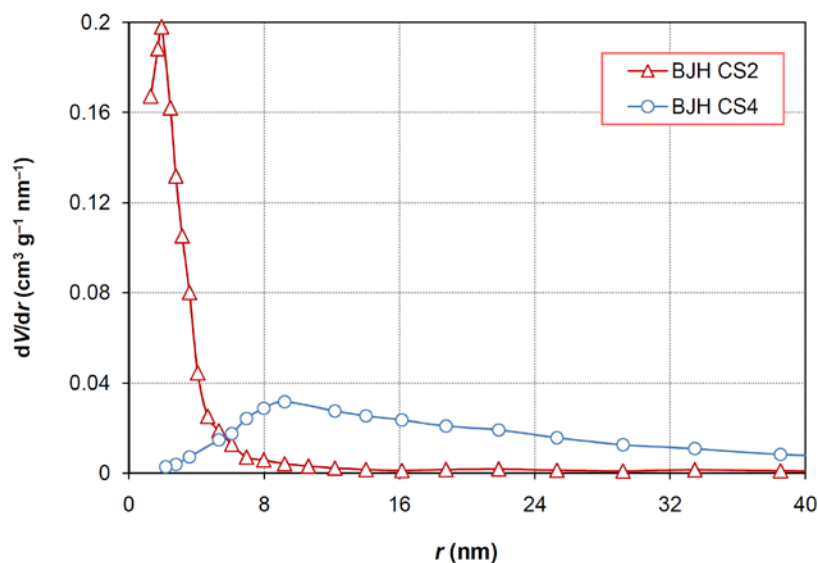


Figure 5. N₂ adsorption-desorption isotherms (upper panel) and BJH plots (lower panel) of CS2 and CS4 catalysts.

The obtained results clearly indicate that both types of synthesized catalysts have an acceptable pore size which in the case of nano-sized support is almost five times larger than that of the porous bulky type. Although this large pore size could prevent any possible blockage, it also might probably reduce the plausibility of effective collisions of reactants with the active surfaces of the catalysts. The high concentration of hydrogen in the present work could effectively eliminate the probability of a pore blockage. It appears, therefore, that one of the reasons of the poor performance of the nano-sized supports could be the lack of enough or efficient collisions between reactants and catalyst surface as a result of large pore sizes (predominantly 9.2 nm) as well as its low surface area (107 m²/g) in comparison with its counterpart. Considering the surface areas of the catalysts with that of the original supports (*vide supra*), especially for the commercial SiO₂, represents that the surface areas of the supports have not reduced significantly during the impregnation. This indicates the successful preparation of the catalysts. In addition, although commercial SiO₂ had a remarkable

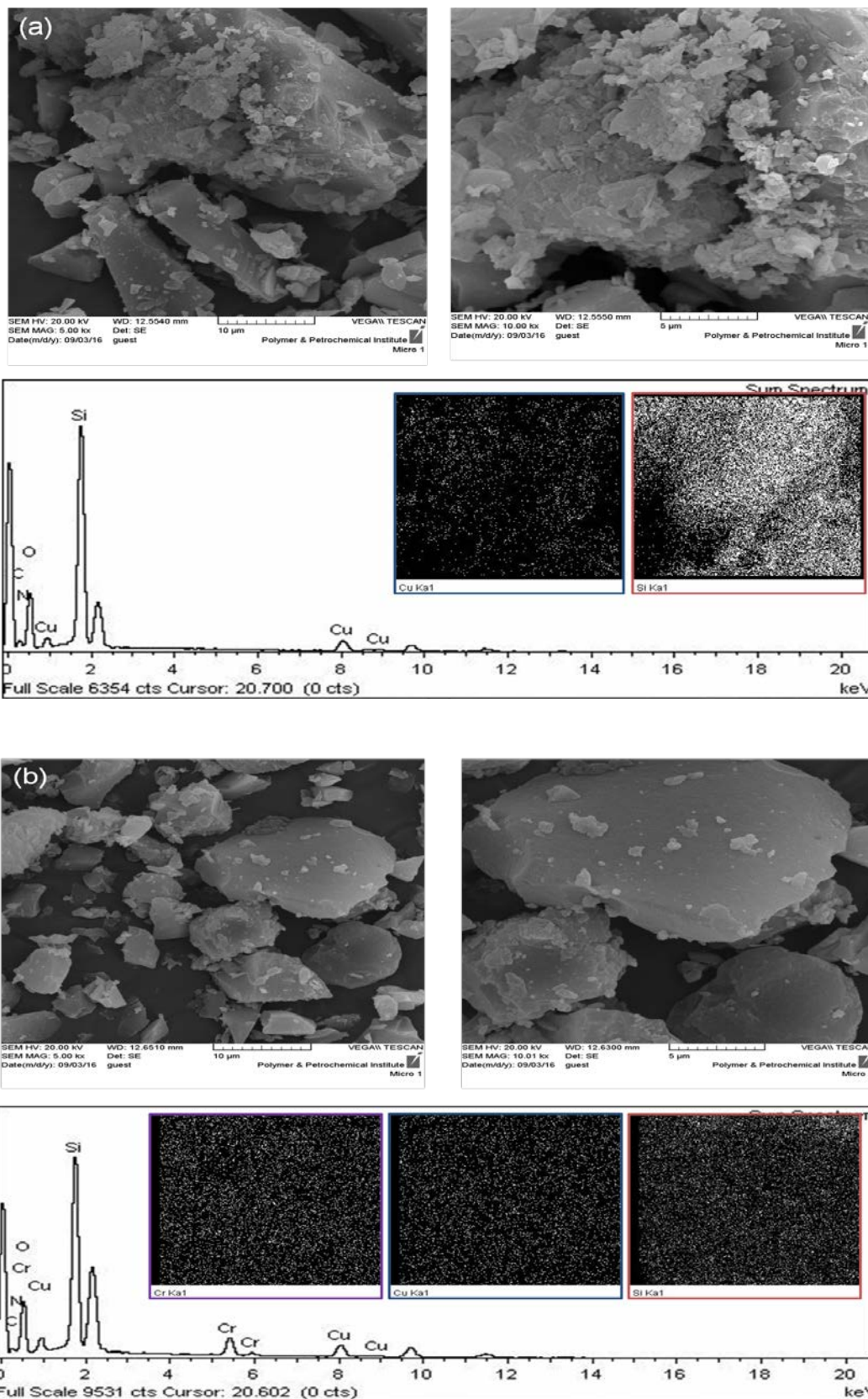
particle size of 34–45 μm, the XRD and isotherm data revealed that it has been effectively formed by the fusion of nano-scaled crystallites while attaining a high internal surface area, which eventually leads to an excellent performance of the resulting catalyst.

The morphologies of the synthesized catalysts are depicted in Fig. 6. All samples showed an aggregate-like morphology. Clearly, the SEM images of CS1 and CS2 are distinguished from those of CS3 and CS4. Larger particles can be detected in the catalysts supported on bulk silica.

Elemental mapping and EDS analyses were also utilized to study the structural features of the catalysts (Fig. 6). The presence of Cu, Si, Cr, C, and O elements in the EDS spectra of all samples was observed. The elemental mapping analyses showed that Cu and Cr in CS2 sample had the best homogeneous dispersion among all of the catalysts. On the basis of the EDS mapping results, the high activity of CS2 can be ascribed to the high dispersion of Cu and Cr on the surface of the bulk-silica support. From these results, one can conclude that a proper dispersion of Cu

and Cr species on the silica support plays a key role in achieving excellent hydrogenation

performances as analogously shown for the case of Cu-B/SiO₂ catalysts [46].



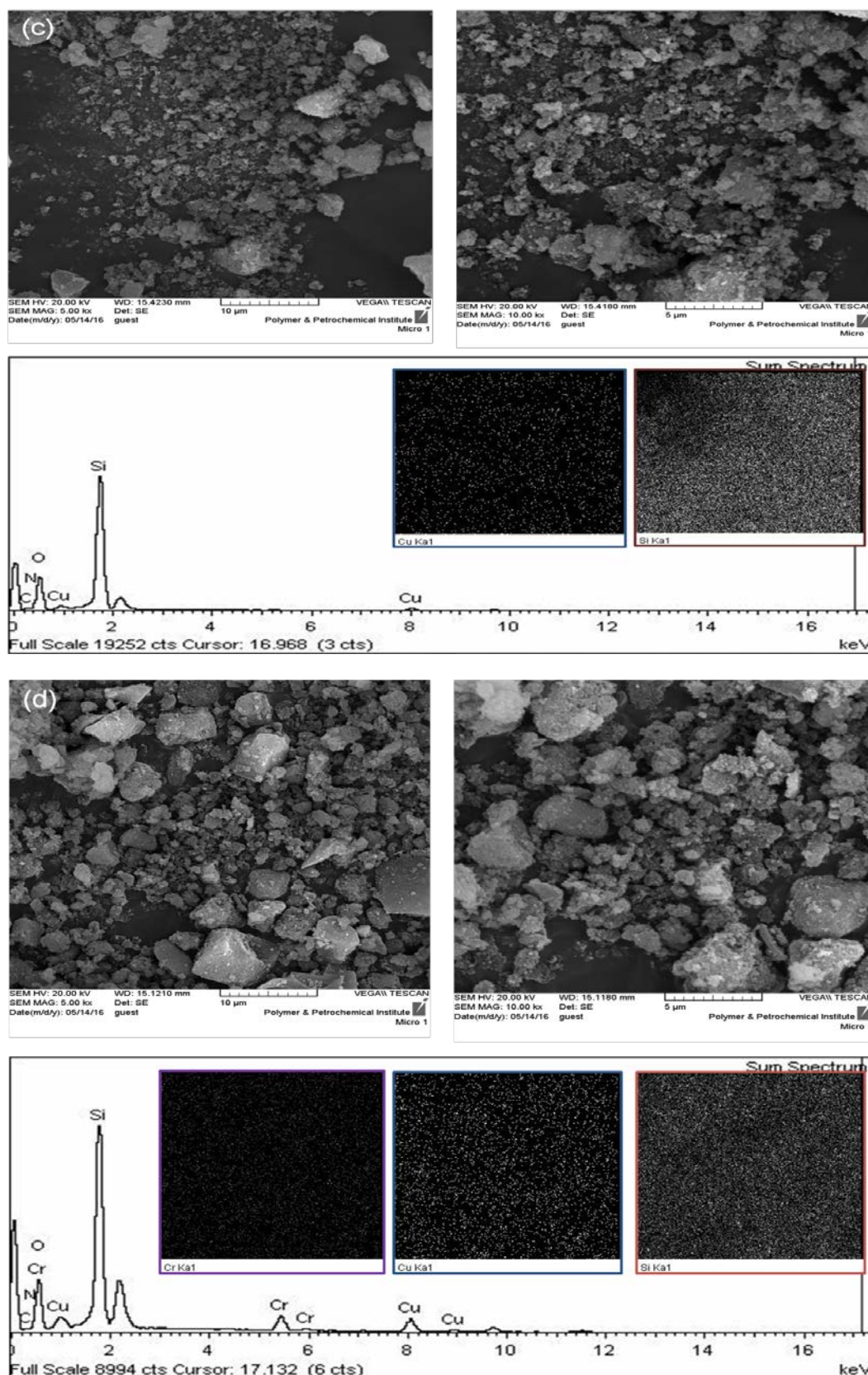


Figure 6. SEM/EDS image of (a) CS1, (b) CS2, (c) CS3 and (d) CS4 catalysts.

4. Conclusions

The copper-catalyzed vapor-phase

hydrogenation of furfural over two types of silica supports (nano-sized and bulk-type)

under mild operating conditions was investigated. The effects of incorporation of a chromium promoter in these two types of catalysts were also assessed. The results revealed that the furfural hydrogenation process over the nano-sized silica-supported catalyst without chromium promoter was more efficient than that on the bulk-type silica particularly in terms of FF conversion and FFA yield. By introduction of chromium as the promoter into the silica-supported copper catalysts, all performance variables (particularly, the FF conversion and FFA yield) improved. This improvement was more intense for the bulk-type silica-supported catalyst. The only disadvantage of this promoter with respect to the catalytic performance of nano-sized silica-supported copper catalyst was a considerable reduction in its durability reflected in the corresponding values of FF conversion and FFA yield. This decrease was not observed in the case of bulk-type silica-supported catalyst, however.

Acknowledgment

The authors appreciate partial support from Iran Polymer and Petrochemical Institute. Thanks are also expressed to Dr. Samahe Sadjadi from IPPI for her kind assistance in this investigation.

References

- [1] Mariscal, R., Maireles-Torres, P., Ojeda, M., Sadaba, I. and Lopez Granados, M., "Furfural: A renewable and versatile platform molecule for the synthesis of chemicals and fuels", *Energ. Environ. Sci.*, **9** (4), 1144 (2016).
- [2] Lange, J.-P., van der Heide, E., van Buijtenen, J. and Price, R., "Furfural: A promising platform for lignocellulosic biofuels", *Chem. Sus. Chem.*, **5** (1), 150 (2012).
- [3] Sun, D., Studies on conversion of biomass-based materials into value-added chemicals, Graduate School of Engineering, Chiba University, (2014).
- [4] Dusselier, M., Mascal, M. and Sels, B., Top chemical opportunities from carbohydrate biomass: A chemist's view of the biorefinery, In: Nicholas, K. M. (Ed.) Selective catalysis for renewable feedstocks and chemicals, Springer International Publishing, (2014).
- [5] Climent, M. J., Corma, A. and Iborra, S., "Conversion of biomass platform molecules into fuel additives and liquid hydrocarbon fuels", *Green Chem.*, **16** (2), 516 (2014).
- [6] Nakagawa, Y., Tamura, M. and Tomishige, K., "Catalytic reduction of biomass-derived furanic compounds with hydrogen", *ACS Catal.*, **3** (12), 2655 (2013).
- [7] Wettstein, S. G., Alonso, D. M., Gürbüz, E. I. and Dumesic, J. A., "A roadmap for conversion of lignocellulosic biomass to chemicals and fuels", *Curr. Opin. Chem. Eng.*, **1** (3), 218 (2012).
- [8] Dutta, S., De, S., Saha, B. and Alam, M. I., "Advances in conversion of hemicellulosic biomass to furfural and upgrading to biofuels", *Catal. Sci. Technol.*, **2** (10), 2025 (2012).
- [9] Corma, A., Iborra, S. and Velty, A., "Chemical routes for the transformation of biomass into chemicals", *Chem. Rev.*, **107** (6), 2411 (2007).
- [10] McMillan, J. D., Biotechnological routes to biomass conversion, DOE/NASULGC Biomass & Solar Energy Workshops, National Bioenergy Center, National Renewable Energy Laboratory, (2004).
- [11] Wu, J., Shena, Y., Liu, C., Wang, H.,

- Geng, C. and Zhang, Z., "Vapor phase hydrogenation of furfural to furfuryl alcohol over environmentally friendly Cu–Ca/SiO₂ catalyst", *Catal. Commun.*, **6** (9), 633 (2005).
- [12] Yan, K., Wu, G., Lafleur, T. and Jarvis, C., "Production, properties and catalytic hydrogenation of furfural to fuel additives and value-added chemicals", *Renew. Sust. Energ. Rev.*, **38**, 663 (2014).
- [13] Hoydonckx, H. E., Van Rhijn, W. M., Van Rhijn, W., De Vos, D. E. and Jacobs, P. A., Furfural and derivatives, In: Ullmann's encyclopedia of industrial chemistry, Wiley Online Library, (2007).
- [14] Li, X., Jia, P. and Wang, T., "Furfural: A promising platform compound for sustainable production of C₄ and C₅ chemicals", *ACS Catal.*, 7621 (2016).
- [15] Nagaraja, B. M., Padmasri, A. H., David Raju, B. and Rama Rao, K. S., "Vapor phase selective hydrogenation of furfural to furfuryl alcohol over Cu–MgO coprecipitated catalysts", *J. Mol. Catal. A*, **265** (1–2), 90 (2007).
- [16] O'Driscoll, Á., Curtin, T., Hernandez, W. Y., Van Der Voort, P. and Leahy, J. J., "Hydrogenation of furfural with a Pt–Sn catalyst: The suitability to sustainable industrial application", *Org. Process Res. Dev.*, **20** (11), 1917 (2016).
- [17] Vetere, V., Merlo, A. B., Ruggera, J. F. and Casella, M. L., "Transition metal-based bimetallic catalysts for the chemoselective hydrogenation of furfuraldehyde", *J. Braz. Chem. Soc.*, **21** (5), 914 (2010).
- [18] Nagaraja, B. M., Aytam, H. P., Podila, S., Reddy, K. H. P., Raju, B. D. and Kamaraju, S. R. R., "A highly active Cu–MgO–Cr₂O₃ catalyst for simultaneous synthesis of furfuryl alcohol and cyclohexanone by a novel coupling route-Combination of furfural hydrogenation and cyclohexanol dehydrogenation", *J. Mol. Catal. A*, **278** (1–2), 29 (2007).
- [19] Ghashghaee, M., Shirvani, S. and Ghambarian, M., "Kinetic models for hydroconversion of furfural over the ecofriendly Cu–MgO catalyst: An experimental and theoretical study", *Appl. Catal. A-Gen.*, **545**, 134 (2017).
- [20] Gao, X., Yu, X., Tao, R. and Peng, L., "Enhanced conversion of furfuryl alcohol to alkyl levulinates catalyzed by synergy of CrCl₃ and H₃PO₄", *BioRes.*, **12** (4), 7642 (2017).
- [21] Shirvani, S. and Ghashghaee, M., "Mechanism discrimination for bimolecular reactions: Revisited with a practical hydrogenation case study", *Phys. Chem. Res.*, **5** (4), 727 (2017).
- [22] Rao, R. S., Baker, R. T. K. and Vannice, M. A., "Furfural hydrogenation over carbon-supported copper", *Catal. Lett.*, **60** (1–2), 51 (1999).
- [23] Nagaraja, B. M., Kumar, V. S., Shasikala, V., Padmasri, A. H., Sreedhar, B., Raju, B. D. and Rao, K. S., "A highly efficient Cu/MgO catalyst for vapour phase hydrogenation of furfural to furfuryl alcohol", *Catal. Commun.*, **4** (6), 287 (2003).
- [24] Reddy, B. M., Reddy, G. K., Rao, K. N., Khan, A. and Ganesh, I., "Silica supported transition metal-based bimetallic catalysts for vapour phase selective hydrogenation of furfuraldehyde", *J. Mol. Catal. A-Chem.*, **265** (1–2), 276 (2007).
- [25] Shirvani, S., Ghashghaee, M., Farzaneh, V. and Sadjadi, S., "Influence of catalyst

- additives on vapor-phase hydrogenation of furfural to furfuryl alcohol on impregnated copper/magnesia”, *Biomass Conv. Bioref.*, **8** (1), 79 (2017).
- [26] Liu, H., Hu, Q., Fan, G., Yang, L. and Li, F., “Surface synergistic effect in well-dispersed Cu/MgO catalysts for highly efficient vapor-phase hydrogenation of carbonyl compounds”, *Catal. Sci. Technol.*, **5** (8), 3960 (2015).
- [27] Baijun, L., Lianhai, L. and Tianxi, C., “Study on selective hydrogenation of furfural to furfuryl alcohol over heteropolyacid modified Raney nickel”, *Chinese J. Catal.*, **3**, (1997).
- [28] Baijun, L., Lianhai, L., Bingchun, W., Tianxi, C. and Iwatani, K., “Liquid phase selective hydrogenation of furfural on Raney nickel modified by impregnation of salts of heteropolyacids”, *Appl. Catal. A-Gen.*, **171** (1), 117 (1998).
- [29] Lee, S.-P. and Chen, Y.-W., “Selective hydrogenation of furfural on Ni-P, Ni-B, and Ni-P-B ultrafine materials”, *Ind. Eng. Chem. Res.*, **38** (7), 2548 (1999).
- [30] Lee, S.-P. and Chen, Y.-W., “Selective hydrogenation of furfural on Ni-P-B nanometals”, *Stud. Surf. Sci. Catal.*, **130**, 3483 (2000).
- [31] Farzaneh, V., Shirvani, S., Sadjadi, S. and Ghashghaee, M., “Promoting effects of calcium on the performance of Cu-MgO catalyst in hydrogenation of furfuraldehyde”, *Iran. J. Catal.*, **7** (1), 53 (2017).
- [32] Ghashghaee, M., Sadjadi, S., Shirvani, S. and Farzaneh, V., “A novel consecutive approach for the preparation of Cu-MgO catalysts with high activity for hydrogenation of furfural to furfuryl alcohol”, *Catal. Lett.*, **147** (2), 318 (2017).
- [33] Sadjadi, S., Farzaneh, V., Shirvani, S. and Ghashghaee, M., “Preparation of Cu-MgO catalysts with different copper precursors and precipitating agents for the vapor-phase hydrogenation of furfural”, *Korean J. Chem. Eng.*, **34** (3), 692 (2017).
- [34] Jiménez-Gómez, C. P., Cecilia, J. A., Durán-Martín, D., Moreno-Tost, R., Santamaría-González, J., Mérida-Robles, J., Mariscal, R. and Maireles-Torres, P., “Gas-phase hydrogenation of furfural to furfuryl alcohol over Cu/ZnO catalysts”, *J. Catal.*, **336**, 107 (2016).
- [35] Li, F., Cao, B., Ma, R., Liang, J., Song, H. and Song, H., “Performance of Cu/TiO₂-SiO₂ catalysts in hydrogenation of furfural to furfuryl alcohol”, *Can. J. Chem. Eng.*, **94** (7), 1368 (2016).
- [36] Ghashghaee, M., Shirvani, S. and Farzaneh, V., “Effect of promoter on selective hydrogenation of furfural over Cu-Cr/TiO₂ catalyst”, *Russ. J. Appl. Chem.*, **90** (2), 304 (2017).
- [37] Wang, Y., Zhou, M., Wang, T. and Xiao, G., “Conversion of furfural to cyclopentanol on Cu/Zn/Al catalysts derived from hydrotalcite-like materials”, *Catal. Lett.*, **145** (8), 1557 (2015).
- [38] Tukacs, J. M., Bohus, M., Dibo, G. and Mika, L. T., “Ruthenium-catalyzed solvent-free conversion of furfural to furfuryl alcohol”, *RSC Adv.*, **7** (6), 3331 (2017).
- [39] Wang, M., Zhang, X., Chen, Z., Tang, Y. and Lei, M., “A theoretical study on the mechanisms of intermolecular hydroacylation of aldehyde catalyzed by neutral and cationic rhodium complexes”, *Sci. China Chem.*, **57** (9), 1264 (2014).

- [40] Vargas-Hernández, D., Rubio-Caballero, J. M., Santamaría-González, J., Moreno-Tost, R., Mérida-Robles, J. M., Pérez-Cruz, M. A., Jiménez-López, A., Hernández-Huesca, R. and Maireles-Torres, P., “Furfuryl alcohol from furfural hydrogenation over copper supported on SBA-15 silica catalysts”, *J. Mol. Catal. A-Chem.*, **383–384**, 106 (2014).
- [41] Sitthisa, S., Sooknoi, T., Ma, Y., Balbuena, P. B. and Resasco, D. E., “Kinetics and mechanism of hydrogenation of furfural on Cu/SiO₂ catalysts”, *J. Catal.*, **277** (1), 1 (2011).
- [42] Villaverde, M. M., Bertero, N. M., Garetto, T. F. and Marchi, A. J., “Selective liquid-phase hydrogenation of furfural to furfuryl alcohol over Cu-based catalysts”, *Catal. Today*, **213**, 87 (2013).
- [43] Aissi, C. F., Daage, M., Wrobel, G., Guelton, M. and Bonnelle, J. P., “Reactive hydrogen species in the copper-chromium oxide system”, *Appl. Catal.*, **3** (2), 187 (1982).
- [44] Wang, S.-R., Yin, Q.-Q. and Li, X.-B., “Catalytic performance and texture of TEOS based Cu/SiO₂ catalysts for hydrogenation of dimethyl oxalate to ethylene glycol”, *Chem. Res. Chin. Univ.*, **28**, 119 (2012).
- [45] Thommes, M., Kaneko, K., Neimark Alexander, V., Olivier James, P., Rodriguez-Reinoso, F., Rouquerol, J. and Sing Kenneth, S. W., “Physisorption of gases, with special reference to the evaluation of surface area and pore size distribution (IUPAC Technical Report)”, *Pure Appl. Chem.*, **87** (9-10), 1051 (2015).
- [46] He, Z., Lin, H., He, P. and Yuan, Y., “Effect of boric oxide doping on the stability and activity of a Cu–SiO₂ catalyst for vapor-phase hydrogenation of dimethyl oxalate to ethylene glycol”, *J. Catal.*, **277** (1), 54 (2011).